Distribution Amplitudes of K^* and ϕ at the Physical Pion Mass from Lattice QCD

Jun Hua,[1] Min-Huan Chu,[1,2] Peng Sun,[3,*] Wei Wang,[1,†] Ji Xu,[1,4] Yi-Bo Yang,[5,6,7] Jian-Hui Zhang,[8] and Qi-An Zhang[2]

(Lattice Parton Collaboration)

[1]*INPAC, Shanghai Key Laboratory for Particle Physics and Cosmology, Key Laboratory for Particle Astrophysics and Cosmology (MOE), School of Physics and Astronomy, Shanghai Jiao Tong University, Shanghai 200240, China*
[2]*Shanghai Key Laboratory for Particle Physics and Cosmology, Key Laboratory for Particle Astrophysics and Cosmology (MOE), Tsung-Dao Lee Institute, Shanghai Jiao Tong University, Shanghai 200240, China*
[3]*Department of Physics and Institute of Theoretical Physics, Nanjing Normal University, Nanjing, Jiangsu 210023, China*
[4]*School of Physics and Microelectronics, Zhengzhou University, Zhengzhou, Henan 450001, China*
[5]*CAS Key Laboratory of Theoretical Physics, Institute of Theoretical Physics, Chinese Academy of Sciences, Beijing 100190, China*
[6]*School of Fundamental Physics and Mathematical Sciences, Hangzhou Institute for Advanced Study, UCAS, Hangzhou 310024, China*
[7]*International Centre for Theoretical Physics Asia-Pacific, Beijing/Hangzhou, China*
[8]*Center of Advanced Quantum Studies, Department of Physics, Beijing Normal University, Beijing 100875, China*

(Received 26 November 2020; accepted 7 July 2021; published 3 August 2021)

We present the first lattice QCD calculation of the distribution amplitudes of longitudinally and transversely polarized vector mesons K^* and ϕ using large momentum effective theory. We use the clover fermion action on three ensembles with $2+1+1$ flavors of highly improved staggered quarks action, generated by the MIMD Lattice Computation Collaboration, at physical pion mass and $\{0.06, 0.09, 0.12\}$ fm lattice spacings and choose three different hadron momenta $P_z = \{1.29, 1.72, 2.15\}$ GeV. The resulting lattice matrix elements are nonperturbatively renormalized in a recently proposed hybrid scheme. An extrapolation to the continuum and infinite momentum limit is carried out. We find that, while the longitudinal distribution amplitudes tend to be close to the asymptotic form, the transverse ones deviate rather significantly from the asymptotic form. Our final results provide crucial *ab initio* theory inputs for analyzing pertinent exclusive processes.

DOI: 10.1103/PhysRevLett.127.062002

Introduction.—Searching for new physics beyond the standard model (SM) is a primary goal of particle physics today. A unique possibility for doing so is to investigate flavor-changing neutral current processes that are highly suppressed in the SM. Some prominent examples of such processes include $B \to K^* \ell^+ \ell^-$ and $B_s \to \phi \ell^+ \ell^-$ decays. Recent experimental analyses by the Belle and LHCb collaborations [1–5] have revealed notable tensions between the SM predictions of such processes and data and attracted quite considerable theoretical interest (see Refs. [6–8] and many references therein). Various new physics interpretations have been proposed to resolve such tensions, but to firmly establish their existence requires an accurate and reliable theoretical understanding of the dynamics of weak decays.

In the low recoil region (high q^2), the $B \to K^*$ and $B_s \to \phi$ form factors can be directly calculated on the lattice (see, for instance, Refs. [9,10]). However, these decays at large recoil are also of experimental interest; for instance, the P_5' anomaly has attracted much theoretical and experimental attention [11,12]. In the latter's kinematics region, decay amplitudes are split into short-distance hard kernels and long-distance universal inputs. The universal inputs that enter include the light-cone distribution amplitudes (LCDAs) of the vector mesons K^*, ϕ which, to leading-twist accuracy, specify the longitudinal momentum distribution among the valence quark and antiquark in the meson. While the hard scattering kernel is perturbatively calculable, the LCDAs can only be extracted from nonperturbative methods or from fits to relevant data. A reliable knowledge of LCDAs is essential in making predictions on physical observables, and in particular the transition form

Published by the American Physical Society under the terms of the Creative Commons Attribution 4.0 International license. Further distribution of this work must maintain attribution to the author(s) and the published article's title, journal citation, and DOI. Funded by SCOAP³.

factors at large recoil can be typically affected by $\mathcal{O}(10\%)$ by the nonasymptotic terms of LCDAs in the light-cone sum rules approach [13,14]. To date most of the available analyses have made use of estimates based on QCD sum rules [15] or Dyson-Schwinger equations [16], but a first-principle description of LCDAs for the vector (K^*, ϕ) meson is still missing.

Lattice QCD provides an ideal *ab initio* tool to access nonperturbative quantities in strong interaction. Though some of the lowest moments of the ρ LCDA have been studied in Ref. [17], a direct calculation of the entire distribution has not been feasible until the recent proposal of a large momentum effective theory (LaMET) [18,19]. This is realized by simulating, on the lattice, appropriately chosen equal-time correlations and then converting them to the LCDAs through a perturbative matching. Since the LaMET was proposed, much progress has been achieved in calculating various parton distribution functions [20,21] (and many references therein) as well as distribution amplitudes for light pseudoscalar mesons [22–24]. Other variants have also been explored in Refs. [25–27].

In this Letter, we present the first lattice calculation of LCDAs for vector mesons K^*, ϕ in LaMET with the clover fermion action on three ensembles with $2+1+1$ flavors of highly improved staggered quarks (HISQ) action [28], generated by MIMD Lattice Computation Collaboration [29], at physical pion mass and $\{0.06, 0.09, \text{and } 0.12\}$ fm lattice spacings. To improve the signal-to-noise ratio of the simulation, we take the smearing transformation of the hypercubic fat link [30]; the other simulation setup is given in Table I. A hybrid renormalization scheme [31] is used to renormalize bare quantities, after which an extrapolation is taken to the continuum limit, as well as to the infinite momentum limit, based on data at three hadron momenta, $P_z = \{1.29, 1.72, 2.15\}$ GeV. It should be noted that a momentum boost close to or larger than the inverse lattice spacing may introduce uncontrolled discretization effects, while the dispersion relation is satisfied with the $\mathcal{O}(a^2)$ corrections, as shown in the Supplemental Material [32]. In the calculation, we neglect the strong decays of K^*, ϕ due to their narrow decay widths. The finite width corrections should be solved with a proper finite-volume analysis, which is beyond the scope of this work. Our final results indicate that, while the longitudinal LCDAs are close to the asymptotic form, the transverse ones deviate considerably from the asymptotic form.

TABLE I. Information on the simulation setup. The light and strange quark mass (both valence and sea quark) of the clover action are tuned such that $m_\pi = 140$ MeV and $m_{\eta_s} = 670$ MeV.

Ensemble	a (fm)	$L^3 \times T$	$c_{\rm SW}$	$m_{u/d}$	m_s
a12m130	0.12	48×64	1.050 88	−0.0785	−0.0191
a09m130	0.09	64×96	1.042 39	−0.0580	−0.0174
a06m130	0.06	96×192	1.034 93	−0.0439	−0.0191

LCDAs from LaMET.—The leading-twist LCDAs for longitudinally and transversely polarized vector mesons, $\Phi_{V,L}$ and $\Phi_{V,T}$, are defined as follows [34]:

$$\int d\xi^- e^{-ixp^+\xi^-} \langle 0|\bar{\psi}_1(0) \not{n}_+ U(0,\xi^-)\psi_2(\xi^-)|V\rangle = f_V n_+ \cdot \epsilon \Phi_{V,L}(x), \tag{1}$$

$$\int d\xi^- e^{-ixp^+\xi^-} \langle 0|\bar{\psi}_1(0) \sigma^{+\mu_\perp} U(0,\xi^-)\psi_2(\xi^-)|V\rangle = f_V^T [\epsilon^+ p^{\mu_\perp} - \epsilon^{\mu_\perp} p^+] \Phi_{V,T}(x), \tag{2}$$

where $U(0,\xi^-) = P\exp[ig_s \int_{\xi^-}^0 ds n_+ \cdot A(sn_+)]$ is the gauge link defined along the minus light-cone direction, ϵ is the polarization vector of the vector meson, and n_+ is the unit vector along the plus light-cone direction. f_V and f_V^T are the decay constants defined by the local vector and tensor current, respectively. Here for K^*, ψ_1 denotes the strange quark field and ψ_2 is the light u/d quark. For the ϕ meson, both $\psi_{1,2}$ are strange quark fields.

According to LaMET, the above LCDAs can be obtained by first calculating the following bare equal-time correlations on the lattice:

$$\begin{aligned} \langle 0|\bar{\psi}_1(0)\gamma^t U(0,z\hat{z})\psi_2(z\hat{z})|V\rangle &= H_{V,L}(z)\epsilon^t f_V, \\ \langle 0|\bar{\psi}_1(0)\sigma_{\nu\rho} U(0,z\hat{z})\psi_2(z\hat{z})|V\rangle &= H_{V,T}(z) f_V^T [\epsilon_\nu p_\rho - \epsilon_\rho p_\nu], \end{aligned} \tag{3}$$

where the Lorentz indices in the second line are chosen as $\{\nu,\rho\} = z, y$, and the gauge link $U(0, z\hat{z})$ is along the z direction. The quantities $H_{V,\{L,T\}}(z)$ can be renormalized nonperturbatively in an appropriate scheme [31,35–40]. Here, we choose the hybrid scheme [31] proposed recently that has the advantage that the renormalization factor does not introduce extra nonperturbative effects at large z that distort the IR property of the bare correlations. This scheme works as follows: At $|z| \le z_S$ where z_S is within the region where the leading-twist approximation is valid, we can choose the regularization-independent momentum subtraction (RI/MOM) scheme [38] to avoid certain discretization effects (alternative choices include, e.g., the ratio [27] scheme), while for $|z| > z_S$ one applies the gauge-link mass subtraction scheme:

$$\begin{aligned} H_V^R(z,a,P_z) = {} & \frac{H_V(z,a,P_z)}{Z(z,a)}\theta(z_S - |z|) \\ & + H_V(z,a,P_z) e^{-\delta m(\tilde{\mu})z} \\ & \times Z_{\rm hybrid}(z_S,a)\theta(|z| - z_S), \end{aligned} \tag{4}$$

where the superscript R denotes the renormalized quantity and $\tilde{\mu}$ denotes the intrinsic scale dependence of the gauge

link, including both UV and IR. We have chosen $Z(z,a)$ as the RI/MOM renormalization factor computed from

$$Z(z,a) = \frac{1}{12}\mathrm{Tr}[\langle S(p)\rangle^{-1} \times \langle S(p|z)\rangle \gamma_z\gamma_5 \times \prod_n U_z(n\hat{z}) S(p|0)\langle S(p)\rangle^{-1}\gamma_z\gamma_5]_{p^2=-\mu_R^2,\, p_z=0}. \quad (5)$$

The Z_{hybrid} denotes the endpoint renormalization constant that can be determined by imposing a continuity condition at $z = z_S$,

$$Z_{\mathrm{hybrid}}(z_S,a) = e^{\delta m(\tilde{\mu})z_S}/Z(z_S,a). \quad (6)$$

The mass counterterm $\delta m(\tilde{\mu})$ can be extracted from the RI/MOM renormalization factor [31]. The z_S are chosen as 0.24 fm and 0.36 fm within the perturbative region, and their difference is treated as a systematic error.

By Fourier transforming $H^R_{V,\{L,T\}}$ to momentum space, we then obtain the quasi-distribution amplitudes (quasi-DAs)

$$\tilde{\Phi}_{V,\{L,T\}}(y,P_z) = \int dz e^{-iyP_z z} H^R_{V,\{L,T\}}(z,P_z), \quad (7)$$

where the continuum limit has been taken. It can be factorized into the LCDAs through the factorization theorem [41]

$$\tilde{\Phi}_{V,\{L,T\}}(y,P_z,\mu_R) = \int_0^1 dx C_{V,\{L,T\}}(x,y,P_z,\mu_R,\mu)\Phi_{V,\{L,T\}}(x,\mu), \quad (8)$$

where the matching kernel $C_{V,\{L,T\}}$ was derived first in the transverse momentum cutoff scheme in Ref. [42] and then in the RI/MOM scheme in Ref. [43]. The μ and μ_R reflect the generic renormalization scale dependence of LCDAs and quasi-DAs. The matching formula and more details of the hybrid scheme can be found in the Supplemental Material [32].

Numerical setup.—On the lattice, one directly calculates the two-point correlation function defined as

$$C_2^m(z,\vec{P},t) = \int d^3y e^{-i\vec{P}\cdot\vec{y}}\langle 0|\bar{\psi}_1(\vec{y},t)\Gamma_1 U(\vec{y},\vec{y}+z\hat{z}) \times \psi_2(\vec{y}+z\hat{z},t)\bar{\psi}_2(0,0)\Gamma_2\psi_1(0,0)|0\rangle, \quad (9)$$

where the longitudinal polarization case ($m = L$) has $\Gamma_1 = \gamma_t$ and $\Gamma_2 = \gamma_z$, and the transverse polarization case ($m = T$) has $\Gamma_1 = \sigma_{zy}$ and $\Gamma_2 = \gamma_x/\gamma_y$. Then, the quasi-DAs can be extracted from the following parameterization:

$$\frac{C_2^m(z,\vec{P},t)}{C_2^m(z=0,\vec{P},t)} = \frac{H^b_{V,m}(z)[1+c_m(z)e^{-\Delta E t}]}{[1+c_m(0)e^{-\Delta E t}]}, \quad (10)$$

where $c_m(z)$ and ΔE are free parameters accounting for the excited state contaminations, and $H^b_{V,m}(z)$ are the bare matrix elements for the quasi-DAs. When t is large enough, the excited state contaminations parameterized by $c_m(z)$ and ΔE are suppressed exponentially, and the ratio defined in Eq. (10) approaches the ground state matrix element $H^b_{V,m}(z)$. Based on the comparison between the joint two-state fit and constant fit shown in the Supplemental Material [32], we choose to use the constant fit in the range of $t \geq 0.54$ fm to provide a conservative error estimate in the following calculation.

The numerical simulation is based on three ensembles with $2+1+1$ flavors of HISQ [28] at a physical pion mass with $\{0.06, 0.09, \text{and } 0.12\}$ fm lattice spacings. The momentum smeared grid source [44] with the source positions $(x_0 + j_x L/2, y_0 + j_y L/2, z_0 + j_z L/2)$ are used in the calculation, where (x_0, y_0, z_0) is a random position and $j_{x,y,z} = 0/1$. It allows us to obtain the even momenta in units of $2\pi/L$ with ~8 times the statistics. We also repeat the calculation at 8, 6, 4 time slices and fold the data in the normal and reversed time directions, which is equivalent to having $570\times8\times8\times2$, $730\times8\times6\times2$, and $970\times8\times4\times2$ measurements at three ensembles at $a = 0.06$, 0.09, and 0.12 fm, respectively. We have further reversed the $\hat{z}$ direction in Eq. (9) to double the statistics. Based on the numerical results, we confirmed that the dispersion relation can be satisfied for all the cases up to the $\mathcal{O}(a^2p^4)$ correction, and the continuum extrapolation in the coordinate space or momentum space provides consistent results [32].

Results.—After renormalization in the hybrid scheme, we perform a phase rotation $e^{izP_z/2}$ to the renormalized correlation, so that the imaginary part directly reflects the flavor asymmetry between the strange and up and down quarks. Taking the transversely polarized K^* as an example, we show in Fig. 1 the real (upper panel) and imaginary part (lower panel) of the renormalized quasi-DA matrix elements $e^{izP_z/2}H_{K^*,T}(z)$ with the momentum $P_z = 2\pi/L \times 10 = 2.15$ GeV. As shown in the upper panel, the matrix elements at different lattice spacings are consistent with each other, indicating that linear divergences arising from the gauge link have been canceled up to the current numerical uncertainty. In the lower panel, we find a positive imaginary part at all the lattice spacings, which corresponds to a nonzero asymmetry with the peak at $x < 1/2$. This is consistent with expectations that lighter quarks carry less momentum of the parent meson.

As one can see from Fig. 1, the uncertainty of the lattice data grows rapidly with the spatial separation of the nonlocal operator. Thus, to have a reasonable control of uncertainties in the final result we need to truncate the correlation at a certain point. The missing long-range information can be supplemented by a physics-based extrapolation proposed in Ref. [31], which removes unphysical oscillations in a naive truncated Fourier transform with the price of altering the

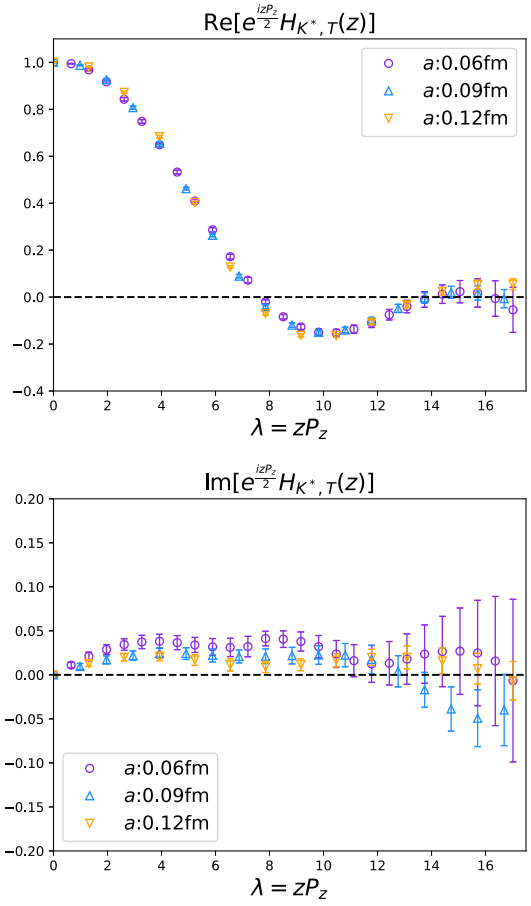

FIG. 1. The two-point correlation function for the transversely polarized K^* in coordinate space. We make a phase rotation by multiplying a factor $e^{izP_z/2}$ with $P_z = 2.15$ GeV.

endpoint distribution (at $x \sim 0$ or 1), which cannot be reliably predicted by LaMET anyway due to increasingly important higher-twist contributions. Following Ref. [31], we adopt the following extrapolation form:

$$H_{V,\{L,T\}}(z, P_z) = \left[\frac{c_1}{(-i\lambda)^a} + e^{i\lambda}\frac{c_2}{(i\lambda)^b}\right] e^{-\lambda/\lambda_0}, \quad (11)$$

where the exponential term accounts for the finite correlation length for a hadron at finite momentum, and the two algebraic terms account for a power law behavior of the momentum distribution at x close to 0 and 1, respectively. $\lambda = zP_z$, and the parameters $c_{1,2}, a, b, \lambda_0$ are determined by a fitting to the lattice data in the region where it exhibits an exponential decay behavior. To account for the systematics from such an extrapolation, we have done two different extrapolations, one including the exponential term and the other not, and taken their difference as an estimate of the systematics. This can be attributed as a source of the uncertainty from the inverse problem, and a more systematic strategy to handle the inverse problem of the Fourier transform is available in Ref. [45]. The detailed

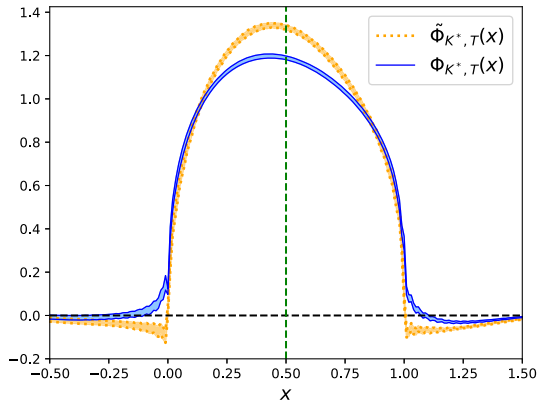

FIG. 2. Quasi-DA and LCDA extracted from it for the transversely polarized K^* using data at $a = 0.09$ fm, $P_z = 2.15$ GeV.

comparison of two extrapolations can be found in the Supplemental Material [32].

After renormalization and extrapolation, we can Fourier transform to momentum space and apply the corresponding matching. In Fig. 2, we show as an example the comparison of the quasi-DA and extracted LCDA for the transversely polarized K^*. The results correspond to the case with $P_z = 2.15$ GeV and $a = 0.09$ fm. One notices that there is a nonvanishing tail for the quasi-DA (yellow curve) in the unphysical region ($x > 1$ or $x < 0$), but it becomes much better for the LCDA (blue curve) after the perturbative matching is applied.

We have performed a simple extrapolation to the continuum limit using the results at three different lattice spacings and the following formula:

$$\psi(a) = \psi(a \to 0) + c_1 a + \mathcal{O}(a^2), \quad (12)$$

with the $\mathcal{O}(a)$ correction being due to the mixed action effect from the clover valence fermion on HISQ sea. As an example, we show the extrapolated results for the transversely polarized K^* in Fig. 3 for three different momenta, $P_z = \{1.29, 1.72, 2.15\}$ GeV. From this figure, one can see that the asymmetry slightly increases with P_z. Defining the asymmetry as $c_{\text{asy}} = \int_0^{1/2} dx\phi(x) / \int_{1/2}^1 dx\phi(x)$, we find c_{asy} is 1.090(15), 1.176(07), and 1.227(08) for the three momenta. Since the strange quark is heavier than the up or down quark, a slight preference of $x < 1/2$ to $x > 1/2$ is expectable. It suggests that a large P_z extrapolation is essential to suppress the power corrections and reproduce this correct preference behavior. Such a behavior is also observed in the study of Kaon LCDAs in Ref. [24].

After matching from quasi-DA to LCDAs with $\mu = 2$ GeV, our final results for LCDAs of the K^* and ϕ are given in Figs. 4 and 5, respectively, where the upper and lower panels correspond to the longitudinal and transverse polarization cases. In these figures, we have made a $P_z \to \infty$ extrapolation using the following simple form:

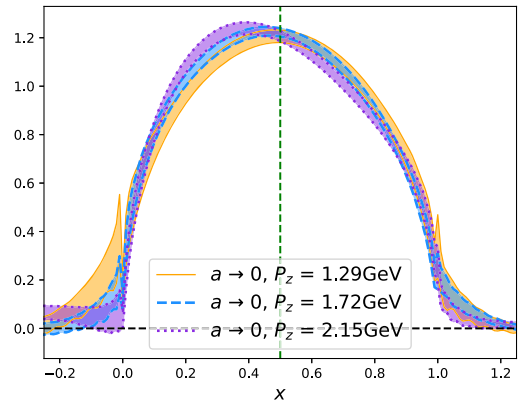

FIG. 3. The continuum limit of the LCDA for the transversely polarized K^*, extrapolated from three different lattice spacings.

$$\psi(P_z) = \psi(P_z \to \infty) + \frac{c_2}{P_z^2} + \mathcal{O}\left(\frac{1}{P_z^4}\right). \tag{13}$$

We have chosen two renormalization scales (1.82 GeV and 3.04 GeV) and treated their difference with an estimate of the systematic error from matching. It is worth emphasizing that the endpoint regions are difficult to access in LaMET. The endpoint can be roughly estimated from the largest attainable λ (conjugate variable of x in the Fourier transform) as $1/\lambda_{\max}$. In the present calculation, we have $\lambda_{\max} \approx 14$ (specifically $z_{\max}^{P_z=1.29\ \mathrm{GeV}} \approx 2.1$ fm, $z_{\max}^{P_z=1.72\ \mathrm{GeV}} \approx 1.6$ fm, $z_{\max}^{P_z=2.15\ \mathrm{GeV}} \approx 1.3$ fm), thus we take a conservative estimate of the predictable region as $[0.1, 0.9]$. Beyond this region, we plot a shaded area with systematic errors difficult to estimate. As a comparison, we also show in Fig. 4 the asymptotic form $6x(1-x)$ and the model results from earlier QCD sum rule calculations [15] and the Dyson-Schwinger equations (DSE) results [16] in Fig. 5. Our results indicate that, while the longitudinal LCDAs tend to be close to the asymptotic form, the transverse LCDAs have relatively large deviations from the asymptotic form. These behaviors might have important implications for the study of semileptonic $B \to K^* \ell^+ \ell^-$ decay toward the search for new physics and can be explored in the future.

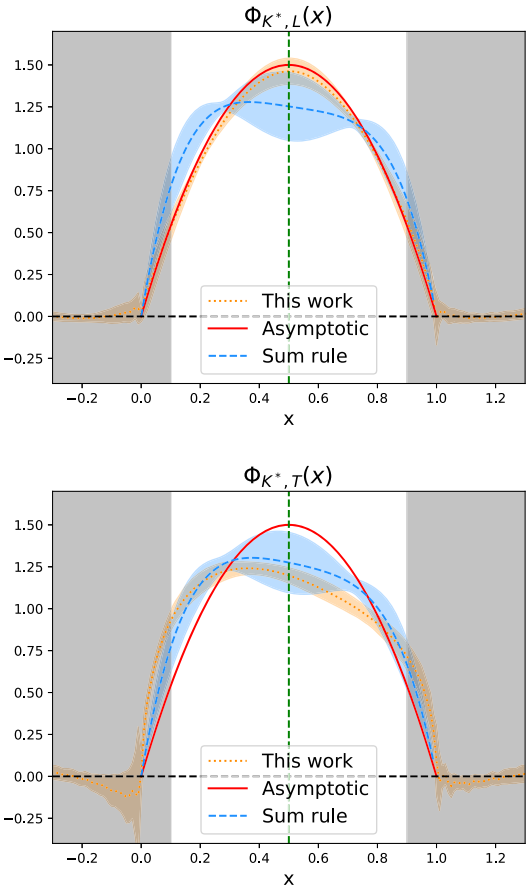

FIG. 4. LCDAs for the longitudinally polarized K^* (upper panel) and transversely polarized K^* (lower panel). The results are extrapolated to the continuous limit ($a \to 0$) and the infinite momentum limit ($P_z \to \infty$). Regions with $x < 0.1$, $x > 0.9$ are shaded, as systematic errors in these regions are difficult to estimate.

Summary.—We have presented the first lattice QCD calculation of LCDAs of longitudinally and transversely polarized vector mesons K^*, ϕ using LaMET. We did not consider the ρ meson due to its large width, which will introduce sizable systematic errors. The continuum and

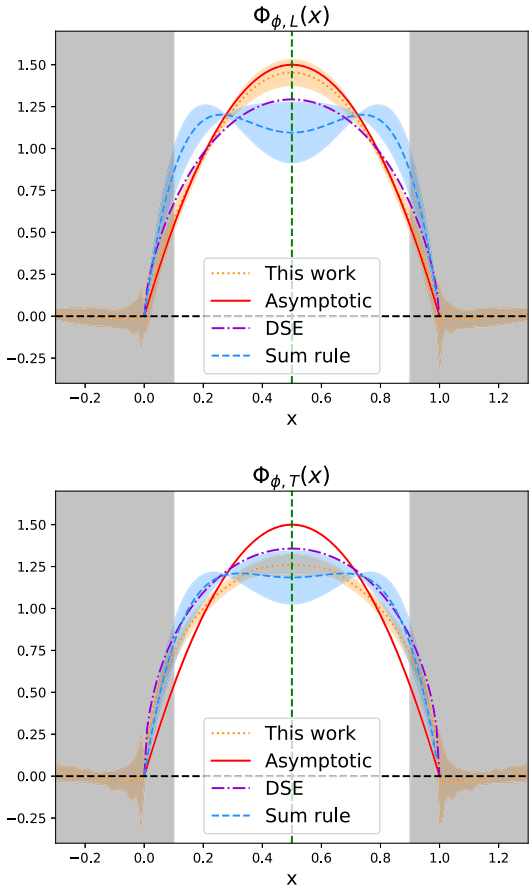

FIG. 5. Similar to Fig. 4 but for the ϕ vector meson.

infinite momentum limits are taken based on calculations at physical light and strange quark mass with three lattice spacings and momenta. Our final results are then compared to the asymptotic form and QCD sum rule results. While the longitudinal LCDAs tend to be close to the asymptotic form, the transverse ones have relatively large deviations from the asymptotic form. Our final results provide crucial *ab initio* theory inputs for analyzing pertinent exclusive processes.

We thank Xiangdong Ji, Liuming Liu, Maximilian Schlemmer, and Andreas Schäfer for valuable discussions. We thank the MIMD Lattice Computation Collaboration for providing us their HISQ gauge configurations. The LQCD calculations were performed using the CHROMA software suite [46] and QUDA [47–49] through the Heterogeneous-Computing Interface for Portability programming model [50]. The numerical calculation has majorly been done on the CAS Xiandao-1 computing environment and supported by the Strategic Priority Research Program of the Chinese Academy of Sciences, Grant No. XDC01040100. The setup for numerical simulations was conducted on the π2.0 cluster supported by the Center for High Performance Computing at Shanghai Jiao Tong University, the HPC Cluster of ITP-CAS, and Jiangsu Key Lab for NSLSCS. J. H., W. W., and J. X. are supported in part by the Natural Science Foundation of China under Grant Nos. 11735010, 11911530088, U2032102, and 11653003 and by the Natural Science Foundation of Shanghai under Grant No. 15DZ2272100. J. H. is supported by NSFC under Grant No. 11947215. P. S. is supported by the Natural Science Foundation of China under Grant No. 11975127 and the Jiangsu Specially Appointed Professor Program. Y. B. Y. is also supported by the Strategic Priority Research Program of Chinese Academy of Sciences, Grants No. XDB34030303 and No. XDPB15. J. H. Z. is supported in part by the National Natural Science Foundation of China under Grant No. 11975051, and by the Fundamental Research Funds for the Central Universities. P. Sun, W. Wang, Y.-B. Yang, and J.-H. Zhang are also supported by a NSFC-DFG joint grant under grant No. 12061131006 and SCHA~~458/22.

*Corresponding author.
06260@njnu.edu.cn
†Corresponding author.
wei.wang@sjtu.edu.cn

[1] J. T. Wei *et al.* (Belle Collaboration) Phys. Rev. Lett. **103**, 171801 (2009).
[2] R. Aaij *et al.* (LHCb Collaboration) J. High Energy Phys. 09 (2015) 179.
[3] R. Aaij *et al.* (LHCb Collaboration) J. High Energy Phys. 02 (2016) 104.
[4] R. Aaij *et al.* (LHCb Collaboration) J. High Energy Phys. 08 (2017) 055.
[5] R. Aaij *et al.* (LHCb Collaboration) Phys. Rev. Lett. **125**, 011802 (2020).
[6] B. Capdevila, A. Crivellin, S. Descotes-Genon, J. Matias, and J. Virto, J. High Energy Phys. 01 (2018) 093.
[7] D. Buttazzo, A. Greljo, G. Isidori, and D. Marzocca, J. High Energy Phys. 11 (2017) 044.
[8] A. Cerri, V. V. Gligorov, S. Malvezzi, J. Martin Camalich, J. Zupan, S. Akar, J. Alimena, B. C. Allanach, W. Altmannshofer, L. Anderlini *et al.*, CERN Yellow Rep. Monogr. **7**, 867 (2019).
[9] R. R. Horgan, Z. Liu, S. Meinel, and M. Wingate, Phys. Rev. D **89**, 094501 (2014).
[10] R. R. Horgan, Z. Liu, S. Meinel, and M. Wingate, Phys. Rev. Lett. **112**, 212003 (2014).
[11] S. Descotes-Genon, J. Matias, M. Ramon, and J. Virto, J. High Energy Phys. 01 (2013) 048.
[12] R. Aaij *et al.* (LHCb Collaboration) J. High Energy Phys. 02 (2016) 104.
[13] P. Ball and V. M. Braun, Phys. Rev. D **55**, 5561 (1997).
[14] P. Ball and R. Zwicky, Phys. Rev. D **71**, 014029 (2005).
[15] P. Ball, V. M. Braun, and A. Lenz, J. High Energy Phys. 08 (2007) 090.
[16] F. Gao, L. Chang, Y. X. Liu, C. D. Roberts, and S. M. Schmidt, Phys. Rev. D **90**, 014011 (2014).
[17] V. M. Braun, P. C. Bruns, S. Collins, J. A. Gracey, M. Gruber, M. Göckeler, F. Hutzler, P. Pérez-Rubio, A. Schäfer, W. Söldner *et al.*, J. High Energy Phys. 04 (2017) 082.
[18] X. Ji, Phys. Rev. Lett. **110**, 262002 (2013).
[19] X. Ji, Sci. China Phys. Mech. Astron. **57**, 1407 (2014).
[20] X. Ji, Y. Liu, Y. S. Liu, J. H. Zhang, and Y. Zhao, arXiv: 2004.03543.
[21] K. Cichy and M. Constantinou, Adv. High Energy Phys. **2019**, 3036904 (2019).
[22] J. H. Zhang, J. W. Chen, X. Ji, L. Jin, and H. W. Lin, Phys. Rev. D **95**, 094514 (2017).
[23] J. H. Zhang *et al.* (LP3 Collaboration) Nucl. Phys. **B939**, 429 (2019).
[24] R. Zhang, C. Honkala, H. W. Lin, and J. W. Chen, Phys. Rev. D **102**, 094519 (2020).
[25] Y. Q. Ma and J. W. Qiu, Phys. Rev. D **98**, 074021 (2018).
[26] Y. Q. Ma and J. W. Qiu, Phys. Rev. Lett. **120**, 022003 (2018).
[27] A. V. Radyushkin, Phys. Rev. D **96**, 034025 (2017).
[28] E. Follana *et al.* (HPQCD and UKQCD Collaborations) Phys. Rev. D **75**, 054502 (2007).
[29] A. Bazavov *et al.* (MILC Collaboration) Phys. Rev. D **87**, 054505 (2013).
[30] A. Hasenfratz and F. Knechtli, Phys. Rev. D **64**, 034504 (2001).
[31] X. Ji, Y. Liu, A. Schäfer, W. Wang, Y. B. Yang, J. H. Zhang, and Y. Zhao, Nucl. Phys. **B964**, 115311 (2021).
[32] See Supplemental Material, which includes Ref. [33], at http://link.aps.org/supplemental/10.1103/PhysRevLett.127.062002 for a collection of perturbative matching kernels and more detailed results.
[33] T. Regge, Nuovo Cimento **14**, 951 (1959).
[34] A. Ali, V. M. Braun, and H. Simma, Z. Phys. C **63**, 437 (1994).

[35] T. Ishikawa, Y. Q. Ma, J. W. Qiu, and S. Yoshida, arXiv: 1609.02018.
[36] J. W. Chen, X. Ji, and J. H. Zhang, Nucl. Phys. **B915**, 1 (2017).
[37] J. Green, K. Jansen, and F. Steffens, Phys. Rev. Lett. **121**, 022004 (2018).
[38] I. W. Stewart and Y. Zhao, Phys. Rev. D **97**, 054512 (2018).
[39] C. Alexandrou, K. Cichy, M. Constantinou, K. Hadjiyiannakou, K. Jansen, H. Panagopoulos, and F. Steffens, Nucl. Phys. **B923**, 394 (2017).
[40] V. M. Braun, A. Vladimirov, and J. H. Zhang, Phys. Rev. D **99**, 014013 (2019).
[41] X. Ji, A. Schäfer, X. Xiong, and J. H. Zhang, Phys. Rev. D **92**, 014039 (2015).
[42] J. Xu, Q. A. Zhang, and S. Zhao, Phys. Rev. D **97**, 114026 (2018).
[43] Y. S. Liu, W. Wang, J. Xu, Q. A. Zhang, S. Zhao, and Y. Zhao, Phys. Rev. D **99**, 094036 (2019).
[44] Y. B. Yang, A. Alexandru, T. Draper, M. Gong, and K. F. Liu, Phys. Rev. D **93**, 034503 (2016).
[45] J. Karpie, K. Orginos, and S. Zafeiropoulos, J. High Energy Phys. 11 (2018) 178.
[46] R. G. Edwards *et al.* (SciDAC, LHPC and UKQCD Collaborations), Nucl. Phys. B, Proc. Suppl. **140**, 832 (2005).
[47] M. A. Clark, R. Babich, K. Barros, R. C. Brower, and C. Rebbi, Comput. Phys. Commun. **181**, 1517 (2010).
[48] R. Babich, M. A. Clark, B. Joo, G. Shi, R. C. Brower, and S. Gottlieb, arXiv:1109.2935.
[49] M. A. Clark, B. Joó, A. Strelchenko, M. Cheng, A. Gambhir, and R. Brower, arXiv:1612.07873.
[50] Y. J. Bi, Y. Xiao, W. Y. Guo, M. Gong, P. Sun, S. Xu, and Y. B. Yang, Proc. Sci., LATTICE2019 (**2020**) 286 [arXiv: 2001.05706].